

# Underestimates of sensible heat flux due to vertical velocity measurement errors in non-orthogonal sonic anemometers<sup>☆</sup>

John M. Frank<sup>a,b,\*</sup>, William J. Massman<sup>a</sup>, Brent E. Ewers<sup>b</sup>

<sup>a</sup> USDA Forest Service, Rocky Mountain Research Station, 240W. Prospect Rd., Fort Collins, CO 80526, USA

<sup>b</sup> Department of Botany and Program in Ecology, University of Wyoming, 1000 E. University Ave., Laramie, WY 82071, USA

## ARTICLE INFO

### Article history:

Received 12 May 2012

Received in revised form 11 October 2012

Accepted 11 November 2012

### Keywords:

Eddy covariance  
Energy balance closure  
Sonic anemometry  
Surface energy balance  
Systematic flux error

## ABSTRACT

Sonic thermometry and anemometry are fundamental to all eddy-covariance studies of surface energy balance. Recent studies have suggested that sonic anemometers with non-orthogonal transducers can underestimate vertical wind velocity ( $w$ ) and sensible heat flux ( $H$ ) when compared to orthogonal designs. In this study we tested whether a non-orthogonal sonic anemometer (CSAT3, Campbell Scientific, Inc.) measures lower  $w$  and  $H$  than an orthogonal sonic anemometer (SATI/3Vx, Applied Technologies, Inc.) and through experimental manipulation we tested if this difference can be attributed to errors in the CSAT3. Four CSAT3s and one SATI/3Vx were mounted symmetrically in a horizontal array on top of the Glacier Lakes Ecosystem Experiments Site (GLEES) AmeriFlux scaffold (southeastern Wyoming, USA) and in close enough proximity to allow covariance measurements between neighboring sonic anemometers. The CSAT3s were paired and measurements of the three orthogonal wind velocities ( $u$ ,  $v$ , and  $w$ ) were tested by alternatively rotating each sonic anemometer 90° around its  $u$ -axis, essentially forcing the sonic  $v$ -axis transducer system to measure  $w$ . Analysis was performed on data corresponding to gusts of wind located within the 15° cone defined around the  $u$ -axis to ensure operation within manufacturer specifications. We found that the CSAT3 measured 8% lower  $H$  than the SATI/3Vx and that was associated with a 6–12% lower measurement of  $w$ . From the CSAT3 manipulations we found  $w$  was underestimated by 6–10% which led directly to an 8–12% underestimate of the kinematic heat flux, the fundamental covariance of  $H$ . These results have implications for ecosystem flux research and the energy imbalance problem considering the prevalence of the CSAT3 and the non-orthogonal sonic anemometer design.

Published by Elsevier B.V.

## 1. Introduction

Within the micrometeorological community a reoccurring theme is the lack of energy balance closure at individual sites, across sites, and across networks where a common thread is turbulent energy fluxes underestimate the available energy (Foken, 2008; Franssen et al., 2010; Oncley et al., 2007; Stannard et al., 1994; Twine et al., 2000; Wilson et al., 2002). Many plausible explanations for this have been proposed ranging from uncertainties in radiation or eddy-covariance flux measurements, the mismatch of measurement areas between flux components, the neglect of energy storage terms, advective flux divergence, and incorrect coordinate systems (Leuning et al., 2012; Mahrt, 1998; Wilson et al., 2002). The role of sonic anemometry as a potential source of the lack of closure

has also been investigated. Mauder et al. (2007) and Loescher et al. (2005) examined the relative difference between instrument models and manufacturers while Gash and Dolman (2003) investigated the role of turbulent wind caused (co)sine errors where the instruments operate at attack angles outside of their optimal range. Unfortunately, for most flux sites few of these explanations can account for the typical 20% biased underestimate of the turbulent flux components of the energy balance (Leuning et al., 2012).

Another possible explanation for the energy balance closure problem could be due to differences in vertical wind velocity ( $w$ ) and sensible heat-flux ( $H$ ) measurements between orthogonal and non-orthogonal sonic anemometers (Kochendorfer et al., 2012). In the traditional orthogonal design the sonic anemometer transducer pairs are 90° to each other and the vertical measurements are truly vertical, while in the non-orthogonal type all transducers are tilted and clustered such that none of the actual measurements, including  $w$ , are simply horizontal or vertical (Fig. 1). Though there are advantages to both designs, orthogonal sonic anemometers are increasingly rare and account for only 13% of the available AmeriFlux network level 2 sites (<http://ameriflux.ornl.gov/>). Orthogonal sensors have been observed to ‘overestimate’  $w$  and  $H$  (Mauder

<sup>☆</sup> This paper was written and prepared by a U.S. Government employee on official time, and therefore it is in the public domain and not subject to copyright.

\* Corresponding author at: USDA Forest Service, 240 W. Prospect Rd., Fort Collins, CO 80526, USA. Tel.: +1 970 498 1319.

E-mail address: [jfrank@fs.fed.us](mailto:jfrank@fs.fed.us) (J.M. Frank).



**Fig. 1.** Photograph of the experimental setup. Position 1 is in the bottom left. The CSAT3 sonic anemometers in positions 2 and 4 are mounted in the horizontal orientation. The  $u$ ,  $v$ , and  $w$  axes are shown in light blue for position 1. (For interpretation of the references to colour in this figure legend, the reader is referred to the web version of this article.)

et al., 2007) when compared to a non-orthogonal standard. But with no compelling evidence to suggest that the orthogonal  $w$  measurement is erroneous, it is entirely possible that instead the majority of eddy-covariance systems which employ the non-orthogonal sonic anemometer underestimate  $w$  and  $H$ .

Here we hypothesize that a non-orthogonal sonic anemometer underestimates  $w$  and  $H$ . With this sensor we expect to observe lower  $w$  and  $H$  in comparison to an orthogonal anemometer. Through experimental manipulation of instrument orientations and consequently measurements of the three orthogonal wind velocities ( $u$ ,  $v$ , and  $w$ ), we predict that rotating a non-orthogonal sonic anemometer  $90^\circ$  around its  $u$ -axis and forcing the  $v$ -axis transducer system to measure the  $w$  wind component will increase the measurement of  $w$ . In concurrence, we also expect a corresponding decrease in the measured  $v$  wind component due to the erroneous sonic  $w$ -axis transducer system measuring the horizontal cross-wind. Finally, we predict that the underestimate in  $w$  also exists in  $H$ , thus yielding a possible explanation for the bias in energy balance closure across a majority of flux sites.

## 2. Methods

### 2.1. Site information and experimental design

Four non-orthogonal (CSAT3, Campbell Scientific Inc., Logan, UT, USA, serial numbers 1046, 1206, 1209, and 1455) and one orthogonal (SATI/3Vx, Applied Technologies Inc., Longmont, CO, USA, serial number 971204, hereafter referred to as the ATI) sonic anemometers were tested in a horizontal array at the top of the Glacier Lakes Ecosystem Experiments Site (GLEES) AmeriFlux scaffold ( $41^\circ 21.992'$  N,  $106^\circ 14.397'$  W, 3190 m above sea level) at an average height of 24.5 m above the soil surface of an 18 m high canopy subalpine forest in southeastern Wyoming, USA described

by Musselman (1994). The sonics were oriented with their azimuth pointed west (or in the case of the ATI, the boom was pointed west) and mounted in five positions located in two rows with the upper row (row 1) 0.35 m above the lower row (row 2). From south to north and relative to position 1 in the lower row, position 2 was 0.35 m north in row 1, position 3 was 0.70 m north in row 2, position 4 was 1.05 m north in row 1, and position 5 was 1.40 m north in row 2 (Fig. 1). The sonics were always mounted such that they were centered at each position and the total distance between adjacent sonic centroids was 0.50 m at a  $45^\circ$  diagonal. The CSAT3s were paired, such that the first pair shared positions 1 and 2 and the second pair shared positions 4 and 5; the ATI was always in position 3. The experiment comprised six stages during an eight week experiment when the pairs of sonics were alternately rotated  $90^\circ$  around their  $u$ -axis into a horizontal orientation such that in sonic coordinates the CSAT3  $w$ -axis was pointing south and the  $v$ -axis was pointing up and the ATI was rotated so its  $w$ -axis was facing north (Table 1). All data are presented in cardinal coordinates ( $u_{\text{cardinal}} = \text{east}$ ,  $v_{\text{cardinal}} = \text{north}$ ,  $w_{\text{cardinal}} = \text{up}$ ) hereby referred to simply as  $u$ ,  $v$ , and  $w$ . The sonic north-south and east-west axes were adjusted to within  $0.4^\circ$  with a digital level while the direction was set by pointing the sonics within  $0.5^\circ$  of a known  $270^\circ$  reference point on the nearby Snowy Range Mountains 4 km away. We marked lines across the side of the CSAT3s for use as guides in sighting horizontally mounted instruments (e.g., the piece of tape on the vertical brace in Fig. 1). Time series data from the five sonics was recorded at 20 Hz on either a CR1000 or CR3000 (Campbell Scientific Inc., Logan, UT, USA). The complete time series was processed (QA/QC) by removing half-hours with physically unrealistic summary statistic measurements (mean, standard deviation, skewness, kurtosis, number of samples) in any of the five sonic anemometers (Vickers and Mahrt, 1997). This amount of processing was deemed sufficient to assure the quality control of the 20 Hz time series samples (Figs. 2 and 3) therefore no despiking algorithm was applied. Finally, since the focus of this study was specifically sonic anemometer measurements, no coordinate rotations, time lag corrections, spectral corrections, or buoyancy corrections were applied to the data.

Non-orthogonal sonic anemometers are most accurate measuring near horizontal winds where transducer shadowing and (co)sine errors are minimized (Gash and Dolman, 2003; Nakai et al., 2006). Similarly, the  $90^\circ$ -rotated horizontal sonic anemometers are most accurate with winds in the vertical plane normal to the sonic  $w$ -axis. In order to facilitate comparisons between simultaneously accurate vertical and horizontal mounted instruments the complete time series data was restricted to gusts of wind within a cone of  $\pm\alpha$  around the  $u$ -axis. Though the CSAT3 has an expected accuracy of 6% for  $\alpha = 20^\circ$  (Campbell Scientific, Inc., 2012), here  $\alpha$  was defined more conservatively at  $15^\circ$  following the results of Kochendorfer et al. (2012). Because many of the wind measurements within the  $15^\circ$  cone were fragmentary and could have been associated with eddies of short length and time scales such that they might not be simultaneously visible to all five sonics, the data was further reduced to gusts of at least a minimum length and hence a minimum time period, defined by Taylor's hypothesis as  $T_i = L/U_i$  where  $T_i$  is the minimum instantaneous time period,  $L$  is the minimum length equal to twice the distance between positions 1 and 5, and  $U_i$  is the instantaneous wind velocity. Then for a series of consecutive 20 Hz sampled wind velocities within the  $15^\circ$  cone, only those series with a minimum of  $2T_{i,\text{max}}f_s$  elements were included in the analysis ( $T_{i,\text{max}}$  is the maximum of the  $T_i$  values within the series,  $f_s$  is the sample rate, and 2 is merely a safety factor). As an example, for a series of 32 consecutive wind velocity measurements within the  $15^\circ$  cone sampled at 20 Hz and  $U_i$  ranging from  $3.7 \text{ m s}^{-1}$  to  $5.0 \text{ m s}^{-1}$ , with  $L = 2.8 \text{ m}$  the maximum  $T_i$  is 0.76 s, and a minimum gust size of  $2 \times 0.76 \times 20 = 30$  samples would be

**Table 1**  
Description of the six different test stages. The subscripts A through D refer to the different CSAT3 sonic anemometers tested. The superscripts denote whether the sonic orientation was V = vertical or H = horizontal. Results for the horizontal oriented ATI are not reported on in this study.

Stage	Dates	Position					Half-hours	Gusts	Samples
		1	2	3	4	5			
		Lower row far south	Upper row near south	Lower row center	Upper row near north	Lower row far north			
1	June 28 to July 5	CSAT3 <sub>A</sub> <sup>V</sup>	CSAT3 <sub>B</sub> <sup>V</sup>	SATI/3Vx <sup>V</sup>	CSAT3 <sub>C</sub> <sup>V</sup>	CSAT3 <sub>D</sub> <sup>V</sup>	254	4072	193,539
2	July 5 to 19	CSAT3 <sub>A</sub> <sup>H</sup>	CSAT3 <sub>B</sub> <sup>V</sup>	SATI/3Vx <sup>H</sup>	CSAT3 <sub>C</sub> <sup>V</sup>	CSAT3 <sub>D</sub> <sup>H</sup>	245	3990	221,303
3	July 19 to 26	CSAT3 <sub>A</sub> <sup>V</sup>	CSAT3 <sub>B</sub> <sup>H</sup>	SATI/3Vx <sup>V</sup>	CSAT3 <sub>C</sub> <sup>H</sup>	CSAT3 <sub>D</sub> <sup>V</sup>	259	5343	254,539
4	July 29 to August 9	CSAT3 <sub>B</sub> <sup>V</sup>	CSAT3 <sub>A</sub> <sup>V</sup>	SATI/3Vx <sup>V</sup>	CSAT3 <sub>B</sub> <sup>V</sup>	CSAT3 <sub>C</sub> <sup>V</sup>	420	9200	423,992
5	August 9 to 16	CSAT3 <sub>B</sub> <sup>H</sup>	CSAT3 <sub>A</sub> <sup>V</sup>	SATI/3Vx <sup>H</sup>	CSAT3 <sub>D</sub> <sup>V</sup>	CSAT3 <sub>C</sub> <sup>H</sup>	280	5315	226,442
6	August 16 to 22	CSAT3 <sub>B</sub> <sup>V</sup>	CSAT3 <sub>A</sub> <sup>H</sup>	SATI/3Vx <sup>V</sup>	CSAT3 <sub>D</sub> <sup>H</sup>	CSAT3 <sub>C</sub> <sup>V</sup>	225	4174	195,889

required for the series to be included in our analysis. A description of the gusts is presented in Section 3.1.

## 2.2. Sensible heat flux measurements with sonic anemometry

Sensible heat flux ( $\text{W m}^{-2}$ ) is defined as

$$H = \rho c_p \overline{w' T'_a} \quad (1)$$

where  $\rho$  ( $\text{kg m}^{-3}$ ) is the air density and  $c_p$  ( $\text{J kg}^{-1} \text{K}^{-1}$ ) is the heat capacity of air while  $\overline{w' T'_a}$  is the kinematic heat flux, which is the covariance of vertical wind velocity ( $\text{m s}^{-1}$ ) and ambient temperature (C) as measured with sonic anemometry. Though sonic

anemometers actually measure sonic virtual temperature,  $T_s$ , ambient temperature fluctuations are easily related to this measurement by  $T'_s = T'_a(1 + \overline{\gamma}_v) + \overline{\gamma}_v T'_a [\rho'_v / \overline{\rho}_v - p'_a / \overline{p}_a]$  where  $\overline{\gamma}_v = (0.32 \overline{p}_v / \overline{p}_a)$ ,  $\rho_v$  is the density of vapor ( $\text{g m}^{-3}$ ),  $p_v$  and  $p_a$  are the partial pressures of vapor and air (kPa), and overbars and primes denote Reynolds decomposition averages and fluctuations (Massman and Lee, 2002). Though they are very similar but not exactly equal, here we focus on  $T_s$  instead of  $T_a$  because it is a fundamental sonic anemometer measurement.

Because horizontally oriented sonics required application of the  $15^\circ$  cone and Reynolds averaging is only valid for continuous data, we analyzed the complete time series data (e.g. no  $15^\circ$  cone applied) only for tests between vertically oriented sonic

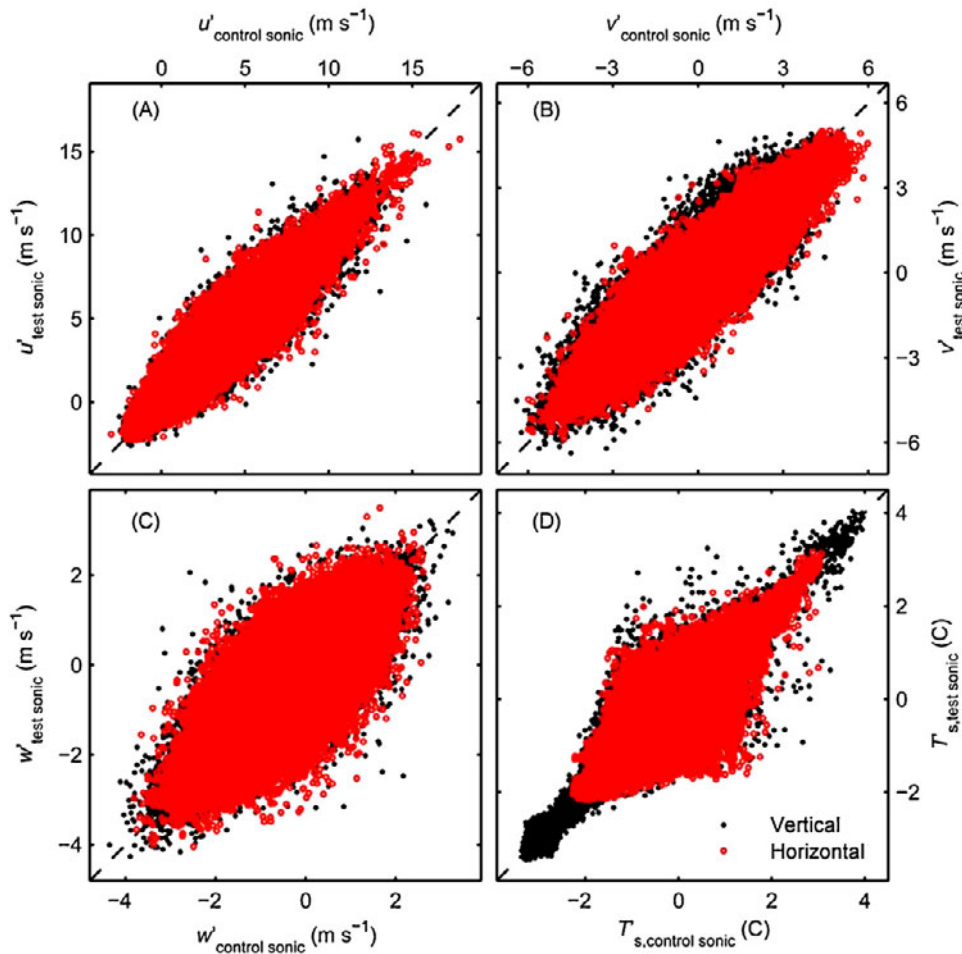


**Fig. 2.** Every sample in the  $15^\circ$  cone comparing measurements from the test sonic anemometers relative to the control sonic anemometers during time when the test sonics were oriented vertical (black, closed circles) or horizontal (red, open circles) for fluctuations of the 3-dimensions of wind velocity ( $u'$ ,  $v'$ , and  $w'$ ) and sonic virtual temperature ( $T_s$ ). (For interpretation of the references to colour in this figure legend, the reader is referred to the web version of this article.)

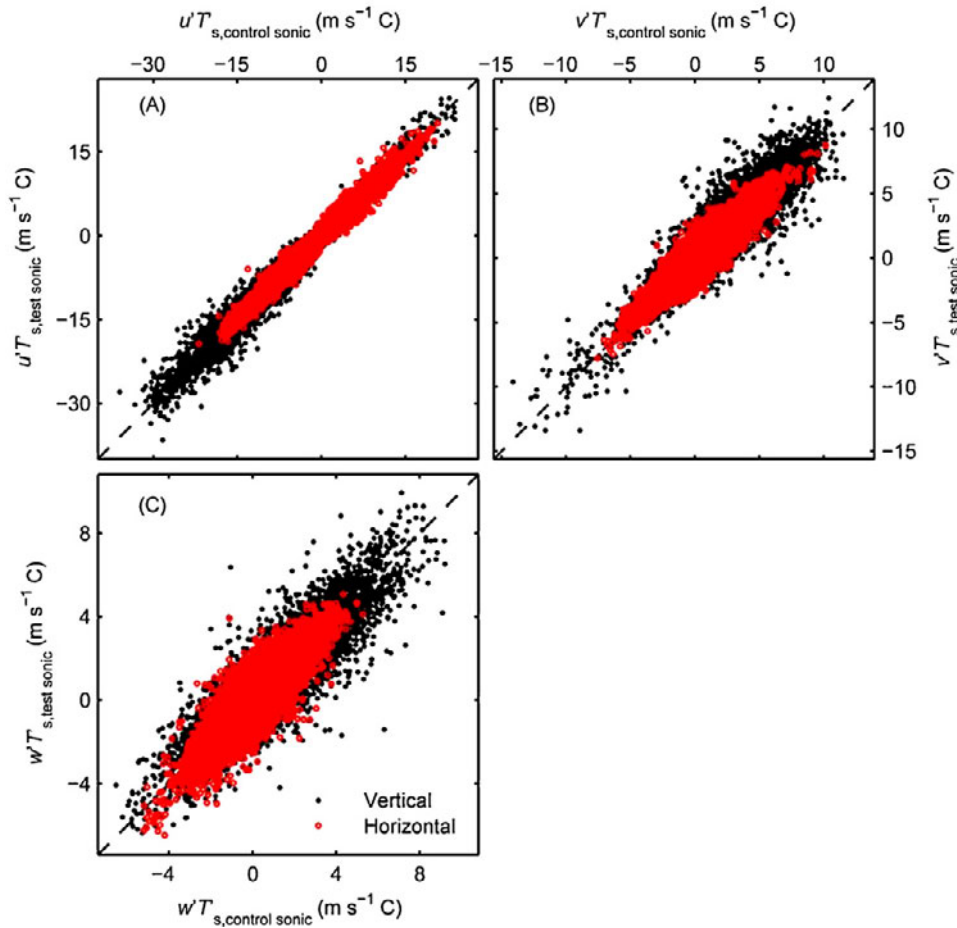


**Fig. 3.** Every sample in the 15° cone comparing measurements from the test sonic anemometers relative to the control sonic anemometers during time when the test sonics were oriented vertical (black, closed circles) or horizontal (red, open circles) for covarying fluctuations of the 3-dimensions of wind velocity ( $u'$ ,  $v'$ , and  $w'$ ) paired with sonic virtual temperature ( $T'_s$ ). To isolate wind velocity measurement errors, all  $T'_s$  values are from the control sonics. (For interpretation of the references to colour in this figure legend, the reader is referred to the web version of this article.)

anemometers, which we limited to comparisons just between the CSAT3 and ATI. We compared these two types of sonic anemometers by using the complete time-series calculated half-hour standard deviations  $\sigma_u$ ,  $\sigma_v$ ,  $\sigma_w$ , and  $\sigma T'_s$ ; covariances  $\sigma T'_s$ ,  $\overline{u'T'_s}$ ,  $\overline{v'T'_s}$ , and  $\overline{w'T'_s}$ ; and sensible heat flux  $H$ . In order to calculate  $H$  additional data processing was required that was not performed elsewhere in our experiment. Before applying Eq. (1) which implicitly includes the humidity or buoyancy correction, data were planar fit rotated (Lee et al., 2004) and spectrally corrected (Massman, 2000; Massman and Clement, 2004) with the required ancillary data taken from the nearby GLEES AmeriFlux eddy-covariance system (Massman and Clement, 2004, <http://ameriflux.ornl.gov/>).

### 2.3. Data analyses

The treatment effect of horizontal versus vertical orientation on the sonic anemometer measurements of the fluctuations  $u'$ ,  $v'$ ,  $w'$ , and  $T'_s$  and covarying fluctuations  $u'T'_s$ ,  $v'T'_s$ , and  $w'T'_s$  was tested by comparing each test sonic relative to its paired and vertically oriented control. To eliminate the possibility of bias, fluctuations were calculated by subtracting the adjusted half-hour average from the corresponding  $u$ ,  $v$ ,  $w$ , or  $T'_s$  measurement on the control sonic from the alternate pair. Adjustments were made based on linear regression between the test or control sonics versus the alternate control sonic. To isolate the horizontal treatment effect on covarying fluctuations due to either wind velocity or sonic temperature, one component was taken from the test sonic while the other

component was held constant on the control sonic. For example, the fluctuations of  $w'$  for CSAT3<sub>A</sub> and CSAT3<sub>B</sub> during stage 2 were calculated as the measurements of  $w$  from the test sonic (1) in position 1 and the control sonic (2) in position 2 while subtracting the adjusted half-hour average of  $w$  from the alternate control sonic (3) in position 4 (Table 1) such that  $w'_{13,i} = w_{1,i} - (\beta_{1,13}\bar{w}_3 + \beta_{0,13})$  and  $w'_{23,i} = w_{2,i} - (\beta_{1,23}\bar{w}_3 + \beta_{0,23})$  for each  $i$ th sample where the  $\beta_s$  are regression parameters between sonics 1 or 2 relative to 3. To test the horizontal treatment effect of  $w'$  on  $w'T'_s$  then  $w'_{13}T'_{23}$  was compared to  $w'_{23}T'_{23}$ . This methodology was also used for comparisons between the CSAT3 and the ATI using the 15°-cone gust data.

Statistical analysis was done using ANCOVA (SAS PROC GLIMMIX, Cary, NC, USA) with the four unique CSAT3s treated as random effects while accounting for autocorrelation of errors in time. All statistical tests included the orientation (vertical or horizontal) of the test sonic. Tests were done with none, one, and two covariates describing the experimental conditions and the half-hour ambient atmospheric conditions measured by the GLEES AmeriFlux eddy-covariance system: row of the test sonic, temperature ( $T_a$ ), pressure, air density ( $\rho_a$ ), vapor density, wind velocity ( $U_a$ ), momentum flux, friction velocity ( $u^*$ ), stability classification (unstable, neutral, stable), stability ( $z/L$ ), 4-way net radiation ( $R_n$ ),  $H$ , latent energy ( $LE$ ), gust size, and time. Models with covariates were ranked using the differences in corrected Akaike's information criteria,  $\Delta AIC_c$  (Akaike, 1974; Burnham and Anderson, 2002). With the extremely large sample size (Table 1) all log likelihood

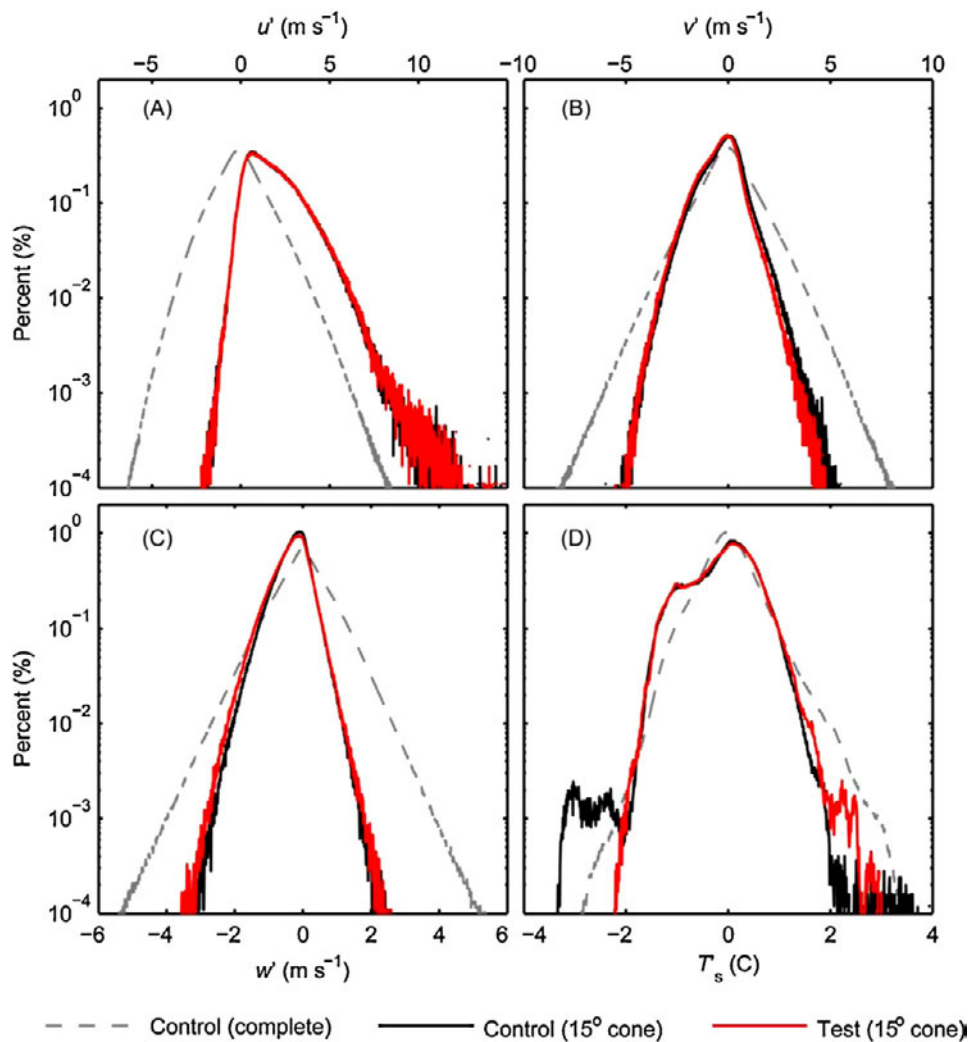


**Fig. 4.** Frequency histograms showing the effect of filtering the complete time series data to restrict winds into the  $15^\circ$  cone for fluctuations of the 3-dimensions of wind velocity ( $u'$ ,  $v'$ , and  $w'$ ) and sonic virtual temperature ( $T_s$ ). Data corresponds to time when the test sonic anemometers were oriented horizontal. Data from the control sonics are shown twice corresponding to the complete time series data (dashed, gray) and the filtered  $15^\circ$ -cone gust data (black). Data from the test sonics are only from the  $15^\circ$ -cone gust data (red). There is a  $-0.1 \text{ m s}^{-1}$  shift in the  $v'$  distribution. Data are binned at  $0.01 \text{ m s}^{-1}$  intervals. (For interpretation of the references to colour in this figure legend, the reader is referred to the web version of this article.)

based criteria are similar and the usual interpretation of the magnitude of AIC differences (Burnham and Anderson, 2002) is not useful because the magnitude of  $\Delta\text{AIC}_c$  between any pair of competing models is  $\gg 10$  (the threshold for essentially no support for a competing model). Instead, as we added covariates to our model we investigated the model with minimum  $\text{AIC}_c$  and in our interpretation looked for compelling qualitative evidence (such as a discernibly large decrease or step down in  $\text{AIC}_c$ ) that it was better than the competing simpler model. Because the test and control sonics were assumed to have equivalent error structures, each model was tested twice: once with the control sonic serving as an independent variable and once with the test sonic considered independent (Meek et al., 1998). For models where the test sonic was an independent variable the regression parameters were inverted. Unless specified, we only report the averages of the parameters from these two models.

### 3. Results

#### 3.1. Description of gusts

During eight weeks in June through August 2011, a total of 32,094 isolated gusts of wind were identified as meeting the criteria

in Section 2.1 (Table 1). These gusts were brief, averaging 2.36 s in duration and ranging from 0.35 s to 41.7 s. They occurred throughout 1683 different half-hours and resulted in 1,515,704 unique measurements for each sonic anemometer (Table 1, Figs. 2 and 3). Measurement errors represented by the CSAT3 diagnostic flags had a minimal impact on our experiment: an *a posteriori* inspection revealed a 0.001% flag rate for the complete time series data and a total of 31 flags set for the  $15^\circ$ -cone gust data. Because of this unusually large sample size, almost every statistical test using the  $15^\circ$ -cone gust data was significant ( $p < 0.0001$ ) in this experiment. Due to these circumstances statistical significance of  $p < 0.0001$  is not necessarily an identifier of meaningful results, so we instead focused on treatment effects with a magnitude  $\geq 2\%$ .

#### 3.2. Distortion caused by the $15^\circ$ -cone requirement

The requirement that wind gusts must be within the  $15^\circ$  cone unfortunately means this subset of data does not necessarily mirror the natural structure of atmospheric turbulence. In all, only 2.5% of the samples in the complete time series data met the criteria for both the  $15^\circ$  cone and the minimum time period. Frequency histograms for the fluctuations and the covarying fluctuations show

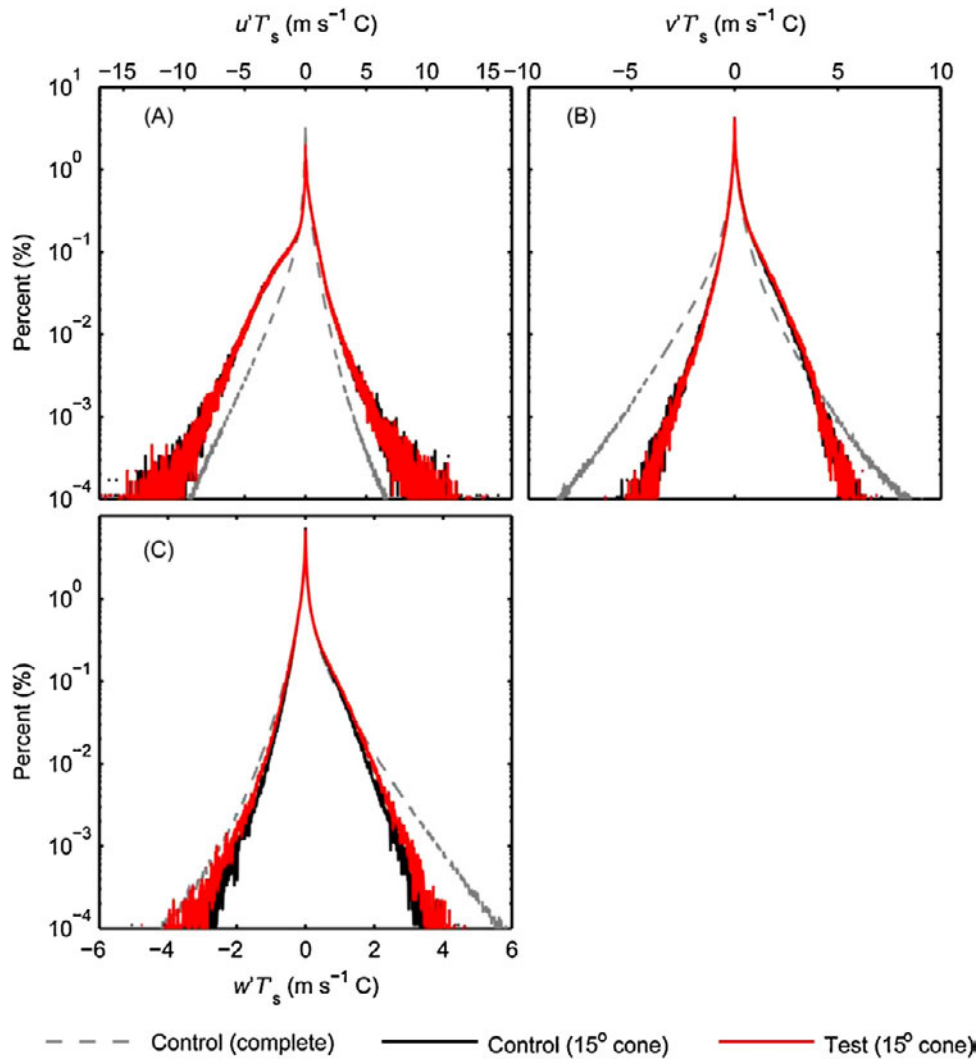


**Fig. 5.** Frequency histograms showing the effect of filtering the complete time series data to restrict winds into the 15° cone for covarying fluctuations of the 3-dimensions of wind velocity ( $u'$ ,  $v'$ , and  $w'$ ) paired with sonic virtual temperature ( $T'_s$ ). Data corresponds to time when the test sonic anemometers were oriented horizontal. To isolate wind velocity measurement errors, all  $T'_s$  values are from the control sonics. Data from the control sonics are shown twice corresponding to the complete time series data (dashed, gray) and the filtered 15°-cone gust data (black). Data from the test sonics are only from the 15°-cone gust data (red). Data are binned at 0.01 m s<sup>-1</sup> C intervals. (For interpretation of the references to colour in this figure legend, the reader is referred to the web version of this article.)

distortions in the natural distributions caused by applying the 15° cone (Figs. 4 and 5). This operation filtered the data such that  $u'$  became almost exclusively positive and the largest values of  $v'$  and  $w'$  were cropped (Fig. 4). The only fluctuation relatively unaffected was  $T'_s$  (Fig. 4). The distributions of the covarying fluctuations  $u'T'_s$ ,  $v'T'_s$ , and  $w'T'_s$  were all less affected by the 15° cone (Fig. 5). The most encouraging was  $w'T'_s$ , which apart from a noticeable reduction in the frequency of covarying fluctuations greater than 2 m s<sup>-1</sup> C, the 15°-cone gust data had a very similar distribution to the complete time series data.

### 3.3. Comparison between the orthogonal and non-orthogonal sonic anemometers

We investigated whether the non-orthogonal CSAT3 underestimated  $w$  and  $H$  relative to the orthogonal ATI. The instruments were compared two ways, both focusing only on sonic anemometers mounted in the vertical orientation. First, using the complete time series data (e.g. no 15° cone applied) the ATI measured 8% higher  $H$  than the CSAT3 ( $p < 0.0001$ , Fig. 6). From Eq. (1) we show that this difference can be traced to a 6% higher  $\sigma_w$  and 11% higher

$\overline{w'T'_s}$  in the ATI ( $p < 0.0001$ , Table 2). Second, focusing only on the 15°-cone gust data, the largest differences were similarly with  $w'$  and  $w'T'_s$  where the ATI was 8% and 12% higher (Table 2). All comparisons involving  $u$  were 3–5% lower in the ATI (Table 2) and were similar for both the complete ( $p < 0.0001$ ) and the 15°-cone data analysis. The comparisons involving  $v$  were highly variable with the ATI between 6% lower and 4% higher than the CSAT3 (Table 2)

**Table 2**

Model slope parameters,  $\beta_1$ , relating the ATI to the CSAT3 for vertically oriented sonic anemometers for the standard deviations ( $\sigma$ ) and covariances (overbars) calculated from the complete times series data and fluctuations ( $'$ ) and covarying fluctuations calculated from the 15° cone gust data for the 3-dimensions of wind velocity ( $u$ ,  $v$ , and  $w$ ) and sonic virtual temperature ( $T_s$ ).  $p < 0.0001$  for all parameters.

Sonic Measurement	$\beta_{1,complete}$	$\beta_{1,15^\circ\text{ cone}}$
$\sigma_u$ or $u'$	0.959	0.950
$\overline{u'T'_s}$ or $u'T'_s$	0.960	0.968
$\sigma_v$ or $v'$	0.994	1.028
$\overline{v'T'_s}$ or $v'T'_s$	0.940	1.037
$\sigma_w$ or $w'$	1.057	1.078
$\overline{w'T'_s}$ or $w'T'_s$	1.109	1.120
$\sigma_{T_s}$ or $T'_s$	1.009	1.041

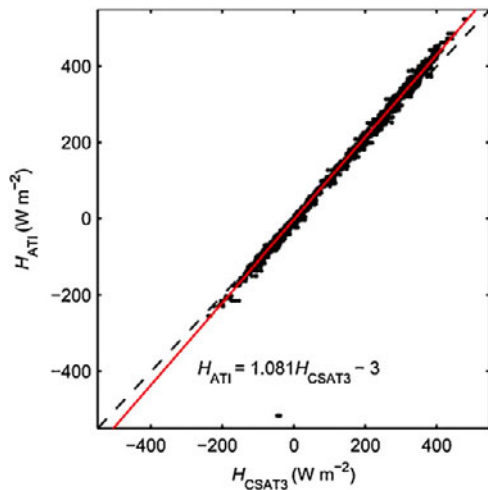


**Fig. 6.** Comparison of half-hour sensible heat flux,  $H$ , between vertically mounted orthogonal (ATI) and four non-orthogonal (CSAT3) sonic anemometers. Outliers corresponding to low  $H_{ATI}$  were not included in the regression (equation, solid red line), but results were similar with their inclusion. (For interpretation of the references to colour in this figure legend, the reader is referred to the web version of this article.)

with the ATI lower in the complete data ( $p < 0.0001$ ) and the ATI higher in the  $15^\circ$ -cone data analysis. Finally,  $\sigma T'_s$  and  $T'_s$  were 1 and 4% higher with the ATI ( $p < 0.0001$ ) (Table 2).

**3.4. Measurement errors within the non-orthogonal sonic anemometer**

We specifically tested if the non-orthogonal CSAT3 underestimated  $w$  and  $H$  by comparing test and control sonic anemometers and measuring how much their relationship changed when the test sonics were rotated to a horizontal position. For this comparison we analyzed the  $15^\circ$ -cone gust data (Figs. 2 and 3). The largest changes detected due to the horizontal treatment were a 7% increase in  $w'$  and an 11% increase in  $w'T'_s$  (Table 3A). By contrast, the treatment effects in  $v'$  (–2%) and  $v'T'_s$  (+3%) were much smaller and were not of consistent signs (Table 3A). This reduction in  $v'$  was confirmed in the frequency histogram (Fig. 4B), along with an unexpected  $-0.1 \text{ m s}^{-1}$  shift in the distribution that was only found in  $v'$ . The effect of the

**Table 3**  
The horizontal orientation treatment effect for the CSAT3: the ratio of the regression slope parameters,  $\beta_1$ , relating the test to the control sonic anemometers for times when the test sonics were oriented H = horizontal versus V = vertical for fluctuations and covarying fluctuations the 3-dimensions of wind velocity ( $u'$ ,  $v'$ , and  $w'$ ) and sonic virtual temperature ( $T'_s$ ) using the  $15^\circ$ -cone gust data. To isolate wind velocity measurement errors in (A) all  $T'_s$  values are from the control sonic. To isolate temperature measurement errors in (B) all wind velocity values are from the control sonic.

(A)	
Sonic measurement	$\beta_{1,H}/\beta_{1,V}$
$u'$	1.004
$u'T'_s$	0.999
$v'$	0.982
$v'T'_s$	1.033
$w'$	1.071
$w'T'_s$	1.109
(B)	
Sonic measurement	$\beta_{1,H}/\beta_{1,V}$
$T'_s$	1.032
$u'T'_s$	1.031
$v'T'_s$	1.032
$w'T'_s$	1.031

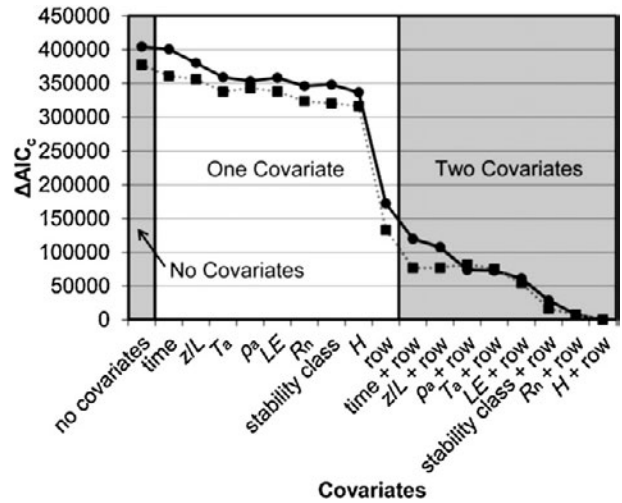


**Fig. 7.** Selection of covariates based on differences in corrected Akaike's information criteria ( $\Delta AIC_c$ ) for the kinematic heat flux ( $w'T'_s$ ) regression for models with different dependent variables:  $w'_{23}T'_{23}$  (solid line) and  $w'_{23}T'_{23}$  (dotted line). Covariates with a minimal change in  $AIC_c$  (less than 25% when compared to the minimum  $AIC_c$ ) among both the one- and two- covariate models are not shown. Covariate symbols are the test-sonic row, ambient temperature ( $T_a$ ), air density ( $\rho_a$ ), stability classification (unstable, neutral, stable), stability ( $z/L$ ), net radiation ( $R_n$ ), sensible heat flux ( $H$ ), and latent heat flux ( $LE$ ).

horizontal treatment on the frequency histogram for  $v'T'_s$  (Fig. 5B) is more difficult to interpret as there are some regions where  $v'T'_s$  appeared to increase and others where it decreased. There was no horizontal treatment effect in  $u'$  or  $u'T'_s$  (Table 3A). And though there was a consistent 3% increase in  $T'_s$  and all of its derived covarying fluctuations with horizontal mounted CSAT3s (Table 3B) we could not determine if this was associated with underestimates in the non-orthogonal design or overestimates in the orthogonal design (Table 2), though Burns et al. (2012) have suggested problems with the  $T'_s$  measurement using the CSAT3 at high wind speeds.

We tested the robustness of these results in the presence of covariates describing the experimental conditions and the half-hour ambient atmospheric conditions. We created models with different combinations of covariates and ranked them by  $\Delta AIC_c$  to qualitatively determine which model was most parsimonious (Fig. 7) and which covariates might influence our analysis. For all tests involving  $u'$ ,  $w'$ ,  $u'T'_s$ , and  $w'T'_s$  (Fig. 7) the single most important covariate was the row where the sonic anemometer was positioned. For  $v'$ ,  $T'_s$ , or  $v'T'_s$  no single covariate stood out, though the lowest  $AIC_c$  occurred with  $U_a$  (for  $v'$  test) or  $H$  (for  $T'_s$  and  $v'T'_s$  tests). For tests involving  $u'$ ,  $w'$ ,  $u'T'_s$ , and  $w'T'_s$  a second covariate was proposed with along with row. None were obviously important (Fig. 7), though  $u'$  (for  $u'$  and  $w'$  tests), time (for  $u'T'_s$  test), and  $H$  (for  $w'T'_s$  test) resulted in the lowest  $AIC_c$ . The horizontal treatment effect in each fluctuation and covarying fluctuation was checked for consistency between the zero, one, and two (where appropriate) covariate models. With the  $w'T'_s$  measurement the horizontal treatment effect was between 8–12% regardless of the inclusion of any covariates (Table 4). Thus, for example, while the row did influence the magnitude of measurements from the test sonic relative to the control sonic ( $\beta_{1,V}$  or  $\beta_{1,H}$  in Table 4) it did not alter the horizontal rotation treatment effect,  $\beta_{1,H}/\beta_{1,V}$ . In general the addition of covariates did not alter the estimated horizontal treatment effects for the other fluctuations and covarying fluctuations. Thus the results in Table 3 are fairly robust, confirming our prediction that  $w'$  measurements increase with a  $90^\circ$  rotation. Among the exceptions was  $w'$ , where the inclusion of row increased the horizontal treatment effect from 7% to 8–10% and the addition of a second covariate yielded a range of 6% to 10%. The inclusion of

**Table 4**

Complete list of parameters solving the model  $w'_{13}T'_{23} = \beta_1 w'_{23}T'_{23} + \beta_0$  for fluctuations vertical wind velocity ( $w'$ ) and sonic virtual temperature ( $T'_s$ ) for V=vertical or H=horizontal oriented test sonic anemometers with zero, one (test-sonic row), and two (test-sonic row and sensible heat flux,  $H$ ) covariates. Subscripts for  $w'$  and  $T'_s$  refer to the fluctuation calculation between either the 1 = test sonic or 2 = control sonic relative to the half-hour average of the 3 = alternate control sonic. The averages of the model results with different dependent variables are in bold. Values for  $H$  represent the 5, 50, and 95% percentiles.

Test-sonic row	$H$ ( $W m^{-2}$ )	$\beta_{1,V}$	$\beta_{0,V}$	$\beta_{1,H}$	$\beta_{0,H}$	$\beta_{1,H}/\beta_{1,V}$	Model dependent variable
n/a	n/a	0.933	-0.05	1.021	-0.04	1.095	$w'_{13}T'_{23}$
		1.087	-0.02	1.219	-0.01	1.121	$w'_{23}T'_{23}$
		<b>1.010</b>	<b>-0.03</b>	<b>1.120</b>	<b>-0.02</b>	<b>1.109</b>	
1	n/a	0.845	0.00	0.929	0.00	1.101	$w'_{13}T'_{23}$
		0.986	0.00	1.076	0.00	1.092	$w'_{23}T'_{23}$
		<b>0.915</b>	<b>0.00</b>	<b>1.003</b>	<b>0.00</b>	<b>1.096</b>	
2		1.027	0.00	1.118	0.01	1.088	$w'_{13}T'_{23}$
		1.176	0.00	1.344	0.00	1.143	$w'_{23}T'_{23}$
		<b>1.101</b>	<b>0.00</b>	<b>1.231</b>	<b>0.00</b>	<b>1.117</b>	
1	-120	0.789	0.01	0.865	0.00	1.097	$w'_{13}T'_{23}$
		1.053	0.04	1.158	0.03	1.100	$w'_{23}T'_{23}$
		<b>0.921</b>	<b>0.02</b>	<b>1.012</b>	<b>0.01</b>	<b>1.099</b>	
2		0.977	-0.02	1.036	-0.05	1.060	$w'_{13}T'_{23}$
		1.263	0.01	1.387	0.00	1.098	$w'_{23}T'_{23}$
		<b>1.120</b>	<b>-0.01</b>	<b>1.211</b>	<b>-0.02</b>	<b>1.082</b>	
1	0	0.812	0.00	0.886	0.00	1.091	$w'_{13}T'_{23}$
		1.045	0.01	1.145	0.00	1.095	$w'_{23}T'_{23}$
		<b>0.929</b>	<b>0.01</b>	<b>1.016</b>	<b>0.00</b>	<b>1.094</b>	
2		0.980	0.00	1.042	-0.01	1.063	$w'_{13}T'_{23}$
		1.229	0.01	1.362	0.01	1.108	$w'_{23}T'_{23}$
		<b>1.104</b>	<b>0.01</b>	<b>1.202</b>	<b>0.00</b>	<b>1.088</b>	
1	380	0.886	-0.02	0.953	0.00	1.075	$w'_{13}T'_{23}$
		1.020	-0.08	1.103	-0.07	1.081	$w'_{23}T'_{23}$
		<b>0.953</b>	<b>-0.05</b>	<b>1.028</b>	<b>-0.03</b>	<b>1.078</b>	
2		0.990	0.08	1.061	0.12	1.072	$w'_{13}T'_{23}$
		1.132	0.02	1.289	0.04	1.139	$w'_{23}T'_{23}$
		<b>1.061</b>	<b>0.05</b>	<b>1.175</b>	<b>0.08</b>	<b>1.108</b>	

covariates for  $v'$  and  $v'T'_s$  tended to decrease their horizontal treatment effect to the ranges -4% to -3% and -3% to 1%. Finally, by adding the covariate for  $T'_s$  or the second covariate for  $u'T'_s$  made the range of their horizontal treatment effects more uncertain ( $\pm 3\%$ ), while the effect for  $T'_s$  decreased toward zero.

**4. Discussion**

*4.1. Is there really a difference in measurements of  $w$  and  $H$  between orthogonal and non-orthogonal sensors?*

We found that either the ATI overestimates both  $w$  and  $H$  or the CSAT3 underestimates them. We found the largest differences between the ATI and the CSAT3 were with  $w$  and  $H$ . Specifically, the CSAT3 measured 8% lower  $w'$ , 6% lower  $\sigma_w$ , 12% lower  $w'T'_s$ , 11% lower  $w'T'_s$  (Table 2), and 8% lower  $H$  (Fig. 6) than the ATI. The differences in  $w'T'_s$  and  $H$  can in part be attributed to the 1% and 4% lower measurements of  $\sigma_{T'_s}$  and  $T'_s$  in the CSAT3 which was not controlled for in those comparisons.

These differences between  $w$  and  $H$  measured with orthogonal versus non-orthogonal sonic anemometers have been observed before. Mauder et al. (2007) performed a field inter-comparison of ten sonic anemometers, including three orthogonal (two type K probes, Applied Technologies and one model TR90-AH, Kaijo-Denki) as well as three CSAT3s, one of which was considered the reference for the study (a different non-orthogonal sonic was used as a reference for one ATI comparison). They found  $\sigma_w$  was anomalously high among the orthogonal sensors (5–6% for the ATIs and 12% for the Kaijo-Denki) as was  $H$  for two of the three orthogonal sensors (8% in one ATI and 22% in the Kaijo-Denki). The only exception was the other ATI, which was interpreted to have normal  $H$  only because of its 3% lower  $\sigma_{T'_s}$  measurement. They interpreted the differences in the Kaijo-Denki as being due to flow interference with a closely mounted krypton hygrometer.

Loescher et al. (2005) also performed a field inter-comparison of eight sonic anemometers including one orthogonal (type K probe, ATI) and one reference CSAT3. Counter to Mauder et al. (2007), their ATI had lower measurements than the CSAT3 for  $\sigma_w$  (0–9%) and  $H$  (7–29%), depending on atmospheric stability and inclusion of a coordinate rotation. This was slightly explained by a 1–4% lower  $\sigma_{T'_s}$  in the ATI. But, considering their ATI's higher  $\sigma_u$  (-3% to 14%) which was unusually large compared to the -4% found in our study (Table 2) or the 3–6% found with  $\bar{u}$  in Mauder et al. (2007), it is possible that the discrepancy in  $H$  between these two studies could be contamination between the  $w'T'_s$  and  $u'T'_s$  signals (Leuning et al., 2012).

This difference has also been observed within the gray literature. First, in 2009 the AmeriFlux portable eddy covariance system (Ocheltree and Loescher, 2007) was deployed at the GLEES site and revealed that  $H$  was 8% higher when measured with an ATI (SATI/3Vx, serial number 971202) relative to the AmeriFlux primary standard CSAT3, and further correspondence confirmed that this difference could not be attributed to buoyancy corrections or coordinate rotations. Second, in a 2010 precursor to this study, we compared two ATIs (the same SATI/3Vx above plus a SATI-3Sx, serial number 021002) to one CSAT3 (one used in this study) and found both ATIs measured higher  $\sigma_w$  (8–9%) and  $H$  (12%) (unpublished data). And finally, Kochendorfer et al. (2012) compared an ATI (SATI/3Vx from this study) to a R.M. Young 81000VRE and found  $\sigma_w$  and  $H$  were 17–14% higher in the ATI.

Though we are not the first to observe that an orthogonal sonic anemometer measures higher  $w$  and  $H$  than a non-orthogonal sensor, we uniquely attempt to determine which instrument is in error. The methodology of Kochendorfer et al. (2012) allowed them to isolate these differences to errors in the non-orthogonal sonic  $w$ . We advance this further by following these errors in  $w$  to errors in the kinematic heat flux, and by implication  $H$ , for a

different non-orthogonal sensor, the more commonly used CSAT3 (<http://ameriflux.ornl.gov/>).

#### 4.2. Interpreting the measurement errors in the non-orthogonal sensor

To evaluate our hypothesis that the CSAT3 underestimates  $w$  and  $H$  measurements, we must determine that the  $\nu$ -axis measurement is correct and that the  $90^\circ$  rotation causes an increase in measured  $w$  and kinematic heat flux along with a corresponding decrease in  $\nu$ .

We did not experimentally test that the  $\nu$ -axis measurement is correct. Quite often this is taken for granted, especially for non-orthogonal omnidirectional sonic anemometers. The CSAT3 accuracy is specified for azimuth angles between  $\pm 170^\circ$  (Campbell Scientific, Inc., 2012). Similarly, Kochendorfer et al. (2012) found no difference in the sonic  $u$  and  $\nu$ -axis with the R.M. Young 81000VRE.

Our data clearly supports the second prediction that rotating the CSAT3 causes an increase in the measured  $w$  wind component. Both  $w'$  and  $w'T'_s$  increased by 7 and 11% with the  $15^\circ$ -cone gust data (Table 3). These results were robust when the analysis included one or two covariates (Fig. 7 and Table 4);  $w'$  increased between 8–10% and 6–10% for the one and two covariate models while  $w'T'_s$  increased between 10–12% and 8–11% similarly. We consistently found this approximately 10% error in  $w'$  and  $w'T'_s$  no matter how we controlled for the possibility of confounding environmental and experimental conditions.

Unfortunately, our data are mixed at best in supporting the final prediction, that rotation causes a corresponding decrease in  $\nu$ . We did detect a small 2% decrease in  $\nu'$ , but it was contradicted by a 3% increase in  $\nu'T'_s$  (Table 3). Though none of the covariates were individually justified, their inclusion did make the horizontal effect more negative for both  $\nu'$  and  $\nu'T'_s$ . We argue, though, that this does not necessarily mean our overall hypothesis is incorrect, rather, it is a question of which is better supported by our data: that  $w'$  and  $w'T'_s$  increased or that  $\nu'$  and  $\nu'T'_s$  did not decrease. It is possible that in our experiment it was much more difficult to detect the rotation effect in the  $\nu$ -axis. There was a  $-0.1 \text{ m s}^{-1}$  shift in the  $\nu'$  measurements associated with horizontal rotation (Fig. 4B) which was not found in either  $u'$  or  $w'$ , which may be an indicator of a larger problem, that being it was more difficult to orient the  $\nu$ -axis correctly. The  $w$ -axis was relatively simple to orient because the CSAT3 could be adjusted with a digital level along both the east-west and north-south axes for both vertical and horizontal orientations. But the  $\nu$ -axis depended on aligning the CSAT3 toward a common landmark on the horizon, which was difficult for the horizontal CSAT3 because there was no natural reference on the instrument with which to sight (Fig. 1). We conducted a sensitivity analysis on our data and found that rotating the horizontal CSAT3s around the  $w$ -axis had a major impact on  $\nu'T'_s$  and changed its horizontal treatment effect by  $-4.5\%$  per  $1^\circ$  of rotation. Hypothetically, with a  $1^\circ$  rotation north the treatment effect in  $\nu'$  and  $\nu'T'_s$  would both decrease and become more similar for both the zero covariate ( $-3\%$  and  $-1\%$ ) and one covariate (ranging from  $-4\%$  to  $-3\%$  in  $\nu'$  compared to  $-4\%$  to  $-2\%$  in  $\nu'T'_s$ ) models with no changes in any of the  $u$  analyses. It is possible using our methodology of aligning the horizontal anemometers that there was a constant bias to the south capable of producing the contradicting  $\nu'$  and  $\nu'T'_s$  results. This leads to a second argument, every model we tested involving  $w$  consistently estimated the measurement to be underestimated by 6–12%, whereas we could not determine if  $\nu$  was consistently underestimated or overestimated. The results for  $w$  were robust even when including covariates while the results for  $\nu$  were not. Third, there could have been interference or crosstalk (Wyngaard, 1988) with the  $\nu'$  measurements because each sonic anemometer was mounted side-to-side by another such that their  $\nu$ -axis were on the same line, while each instrument was

mounted with its own unique  $w$ -axis (Fig. 1). Finally, the frequency histograms in Figs. 4 and 5 illustrate the differences in the composition of the complete time series and the  $15^\circ$ -cone gust data, and the best among these was the  $w'T'_s$  distribution (Fig. 5C). Thus, we contend that the observed  $w'T'_s$  values more likely reflect natural atmospheric conditions than  $\nu'T'_s$ .

#### 4.3. Implications for surface energy imbalance problem

Leuning et al. (2012) found that only 8% of the La Thuile dataset had an energy balance closure; most sites achieve only 80% closure biased toward underestimates of turbulent fluxes (Foken, 2008). An investigation of all available AmeriFlux L2 sites showed that 87% employed non-orthogonal sonic anemometers of which 42% were manufactured by Gill (Hampshire, UK), 35% were the CSAT3, and 18% the model 81000 (R.M. Young) while only 13% used orthogonal sonic anemometers (all ATI, type K probe or 3Vx) (<http://ameriflux.ornl.gov/>). Our results have direct implications for the third of all sites that use the CSAT3 as we found evidence that the CSAT3 underestimates  $w$  and  $H$  by 10%. Combining this with the findings of Kochendorfer et al. (2012) who found the R.M. Young also underestimated  $w$  by 10%, leads to 53% of all AmeriFlux L2 sites using sonic anemometers that have been implicated in underestimating  $w$  and  $H$ . Like Kochendorfer et al. (2012), we similarly argue that underestimates in  $w$  should affect all ecosystem fluxes based on covariances with vertical wind velocity. This can be deduced for  $H$  through commutativity in Eq. 1 and is shown in the similarity of errors in  $w$  and  $w'T'_s$  in Table 3A. This logic is even more evident in Table 3B where the same 3% error in  $T'_s$  appears in all of its covarying fluctuations. Though it was possible that the eddies involved with the errors in  $w$  might not be the same eddies responsible for the transport of energy and mass with in the ecosystem, our results suggest that they are similar because we observed that errors in  $w$  transfer to  $H$ . Thus, since errors in vertical wind velocity would also propagate to vapor flux calculations (see Massman and Lee (2002) for equations) we expect that these errors in  $w$  extend to latent heat fluxes as well. By this same argument, our findings also have implications for eddy-covariance measurements of the net ecosystem exchange of  $\text{CO}_2$  and ecosystem carbon balance.

Recently, there have been several investigations of angle of attack or (co)sine response errors in sonic anemometers (Kochendorfer et al., 2012; Nakai and Shimoyama, 2012; Nakai et al., 2006; van der Molen et al., 2004) and where our findings fit into this context merits discussion. We propose our results are an extension of this work but unique for small angles of attack,  $\alpha$ . In van der Molen et al. (2004), Nakai et al. (2006), and Nakai and Shimoyama (2012),  $w$  corrections were secondary and consequential to correcting the wind data to have an ideal sine response. Because of this, the actual  $w$  corrections were either unstable for small angles of attack (undefined at  $\alpha \approx -0.64^\circ$  for van der Molen et al. (2004) and  $\alpha \approx -1.22^\circ$  for Nakai et al. (2006)) or forced to one for  $\alpha = 0$  (Nakai and Shimoyama, 2012)). Yet, no inferences can be made from any of these studies concerning actual  $w$  errors for  $|\alpha| < 10^\circ$ . Kochendorfer et al. (2012) did find  $w$  errors existed at  $|\alpha| = 5^\circ$ . In our experiment we did not fix the angle of attack, but rather limited it to  $|\alpha| < 15^\circ$ , and as such 96% of the angles of attack tested in our study occurred for  $|\alpha| < 10^\circ$  and 66% for  $|\alpha| < 5^\circ$ . Yet, there were similarities in observed  $w$  errors between all of these studies: Nakai and Shimoyama (2012) found  $w$  was underestimated by 12% for  $\alpha = -10^\circ$ , Kochendorfer et al. (2012) observed 16% and 10% underestimates for  $\alpha = -5^\circ$  and  $5^\circ$ , and we found a 6–10% underestimate for  $|\alpha| < 15^\circ$ . But, unlike the  $w$  correction in Nakai and Shimoyama (2012) which is assumed to approach unity at  $\alpha = 0$ , our results corroborate the assumption of Kochendorfer et al. (2012) that as  $\alpha$  approaches zero the  $w$  correction should remain greater than one. We propose that corrections for  $w$  would

be more accurate, especially for small  $\alpha$ , if they were empirically fit to the relative error in  $w$  and not the deviation from the ideal sine response, which masks the error in  $w$  as  $\alpha$  approaches zero.

Finally, we propose the possibility that this underestimate in  $w$  and  $H$  might not be a manufacturer or sensor specific problem, but rather is a fundamental difference between the orthogonal versus non-orthogonal sensor design. Combining our results for the CSAT3, Kochendorfer et al. (2012) for the R.M. Young, and Mauder et al. (2007) who found similar differences in  $H$  between orthogonal (including an ATI) and non-orthogonal (including the CSAT3 and Gill) sonic anemometers leads us to recognize this possibility. The observations of Nakai and Shimoyama (2012), though not a comparison between different models, are nevertheless consistent with underestimates of  $w$  in the Gill anemometer. One explanation could be that transducer shadowing is minimized with a purely vertical  $w$ -axis thus leading to improved  $w$  measurements with orthogonal sonic anemometers (Kochendorfer et al., 2012). If this were the case, then a fundamental underestimate of  $w$  by non-orthogonal sensors could account for 10% better energy balance closure at 87% of the AmeriFlux sites.

## 5. Conclusions

In this study we found that the largest differences between a non-orthogonal sonic anemometer (CSAT3) and an orthogonal sonic anemometer (SATI/3Vx) were lower CSAT3 measurements of  $w'$  (8%),  $\sigma_w$  (6%),  $w'T'_s$  (12%),  $\overline{w'T'_s}$  (11%), and  $H$  (8%). By experimentally manipulating the CSAT3, we determined that the non-orthogonal sonic underestimated measurements of  $w'$  (6–10%) and  $w'T'_s$  (8–12%). These results suggest that the CSAT3 underestimates  $w$  and  $H$  by about 10%. This is directly applicable to the 35% of all AmeriFlux L2 sites that employ the CSAT3, but it is possible that this problem is inherent to the non-orthogonal sonic anemometer design. Because we observed errors in  $w$  propagating to  $H$ , we deduce that these errors should exist in latent heat and other ecosystem fluxes involving eddy transport of mass or energy. This also clarifies the behavior of the correction in  $w$  relative to (co)sine errors for small angles of attack. These findings could be far reaching by impacting a majority of sites and their ability to measure ecosystem fluxes and achieve energy balance closure.

## Acknowledgements

This work was funded by the U. S. Forest Service, Rocky Mountain Research Station with additional funding from the Wyoming Water Development Commission and USGS. We thank James Kathilankal and AmeriFlux for their intercomparison that brought our attention to this question; Herb Zimmerman at Applied Technologies, Inc., and Ed Swiatek and Larry Jacobsen at Campbell Scientific, Inc. for their expert knowledge and advice with sonic anemometers as well as suggestions to improve our experimental design; and the editor, two reviewers, and Tom Horst for their improvements to this manuscript.

## References

Akaike, H., 1974. A new look at the statistical model identification. *IEEE Trans. Automat. Control* 19 (6), 716–723.

- Burnham, K.P., Anderson, D.R., 2002. Model Selection and Multimodel Inference a Practical Information-Theoretic Approach. Springer eBook collection. New York, Springer.
- Burns, S.P., Horst, T.W., Blanken, P.D., Monson, R.K., 2012. Using sonic anemometer temperature to measure sensible heat flux in strong winds. *Atmos. Meas. Tech. Discuss.* 5 (1), 447–469.
- Campbell Scientific, Inc., 2012. CSAT3 three dimensional sonic anemometer, pp. 72. Foken, T., 2008. The energy balance closure problem: an overview. *Ecol. Appl.* 18 (6), 1351–1367.
- Franssen, H.J.H., Stockli, R., Lehner, I., Rotenberg, E., Seneviratne, S.I., 2010. Energy balance closure of eddy-covariance data: a multisite analysis for European FLUXNET stations. *Agr. Forest Meteorol.* 150 (12), 1553–1567.
- Gash, J.H.C., Dolman, A.J., 2003. Sonic anemometer (co)sine response and flux measurement I. The potential for (co)sine error to affect sonic anemometer-based flux measurements. *Agr. Forest Meteorol.* 119 (3–4), 195–207.
- Kochendorfer, J.P., Meyers, T.P., Frank, J.M., Massman, W.J., Heuer, M.W., 2012. How well can we measure the vertical wind speed? Implications for fluxes of energy and mass. *Boundary-Layer Meteorol.* 145 (2), 383–398.
- Lee, X., Finnigan, J.J., Paw, U.K.T., 2004. Coordinate system and flux bias error. In: Lee, X., Massman, W.J., Law, B.E. (Eds.), *Handbook of Micrometeorology*. Kluwer Academic Publishers, Dordrecht, The Netherlands, pp. 33–66.
- Leuning, R., van Gorsel, E., Massman, W.J., Isaac, P.R., 2012. Reflections on the surface energy imbalance problem. *Agr. Forest Meteorol.* 156, 65–74.
- Loescher, H.W., et al., 2005. Comparison of temperature and wind statistics in contrasting environments among different sonic anemometer-thermometers. *Agr. Forest Meteorol.* 133 (1–4), 119–139.
- Mahrt, L., 1998. Flux sampling errors for aircraft and towers. *J. Atmos. Ocean. Technol.* 15 (2), 416–429.
- Massman, W.J., 2000. A simple method for estimating frequency response corrections for eddy covariance systems. *Agr. Forest Meteorol.* 104 (3), 185–198.
- Massman, W.J., Clement, R., 2004. Uncertainty in eddy covariance flux estimates resulting from spectral attenuation. In: Lee, X., Massman, W.J., Law, B.E. (Eds.), *Handbook of Micrometeorology*. Atmospheric and Oceanographic Sciences Library. Kluwer Academic Publishers, Dordrecht, The Netherlands, pp. 67–99.
- Massman, W.J., Lee, X., 2002. Eddy covariance flux corrections and uncertainties in long-term studies of carbon and energy exchanges. *Agr. Forest Meteorol.* 113 (1–4), 121–144.
- Mauder, M., et al., 2007. The energy balance experiment EBEX-2000. Part II: Intercomparison of eddy-covariance sensors and post-field data processing methods. *Boundary-Layer Meteorol.* 123 (1), 29–54.
- MEEK, D.W., Prueger, J.H., Sauer, T.J., 1998. Solutions for three regression problems commonly found in meteorological data analysis. In: Strand, J.F., Goens, D.W. (Eds.), 23rd Conference on Agricultural Forest Meteorology. American Meteorological Society, Albuquerque, NM, pp. 141–145.
- Musselman, R.C., 1994. The Glacier Lakes Ecosystem Experiments Site. USDA Forest Service, Rocky Mountain Forest and Range Experiment Station, Fort Collins, CO. General Technical Report RM-249.
- Nakai, T. and Shimoyama, K., 2012. Ultrasonic anemometer angle of attack errors under turbulent conditions. *Agricultural and Forest Meteorology*, 162–163(0): 14–26.
- Nakai, T., van der Molen, M.K., Gash, J.H.C., Kodama, Y., 2006. Correction of sonic anemometer angle of attack errors. *Agr. Forest Meteorol.* 136 (1–2), 19–30.
- Ocheltree, T.W., Loescher, H.W., 2007. Design of the AmeriFlux portable eddy covariance system and uncertainty analysis of carbon measurements. *J. Atmos. Ocean. Technol.* 24 (8), 1389–1406.
- Oncley, S., et al., 2007. The energy balance experiment EBEX-2000. Part I: overview and energy balance. *Boundary-Layer Meteorol.* 123 (1), 1–28.
- Stannard, D.I., et al., 1994. Interpretation of surface flux measurements in heterogeneous terrain during the Monsoon '90 experiment. *Water Resour. Res.* 30 (5), 1227–1239.
- Twine, T.E., et al., 2000. Correcting eddy-covariance flux underestimates over a grassland. *Agr. Forest Meteorol.* 103 (3), 279–300.
- van der Molen, M.K., Gash, J.H.C., Elbers, J.A., 2004. Sonic anemometer (co)sine response and flux measurement - II. The effect of introducing an angle of attack dependent calibration. *Agr. Forest Meteorol.* 122 (1–2), 95–109.
- Vickers, D., Mahrt, L., 1997. Quality control and flux sampling problems for tower and aircraft data. *J. Atmos. Ocean. Technol.* 14 (3), 512–526.
- Wilson, K., et al., 2002. Energy balance closure at FLUXNET sites. *Agr. Forest Meteorol.* 113 (1–4), 223–243.
- Wyngaard, J.C., 1988. Flow-distortion effects on scalar flux measurements in the surface layer: Implications for sensor design. *Boundary-Layer Meteorol.* 42 (1), 19–26.